Available online at www.sciencedirect.com
SCIENCE DIRECT
Catalysis Today 101 (2005) 109–116
CATALYSIS TODAY
www.elsevier.com/locate/cattod

New iron containing mesoporous catalysts

Maciej Trejda, Maria Ziolek *

A. Mickiewicz University, Faculty of Chemistry, Grunwaldzka 6, PL-60-780 Poznan, Poland

Available online 7 March 2005

Abstract

Ferroceneacetic acid (FAA) was immobilised on protonated MCM-41, AlMCM-41, NbMCM-41 and amorphous silica. The organometallic complex is anchored to the surface by the interaction with hydroxyl groups and/or niobium species in case of NbMCM-41 support. Thermal stability of ferrocene species immobilised on the solid surface is not significantly influenced by the nature and composition of the matrix contrary to leaching behaviour, which is higher in case of NbMCM-41 and silica supports. The feature of these solids as catalysts has been estimated in the hydroxylation/polymerisation of phenol and decomposition of isopropanol. In the latter reaction the redox properties are slightly pointed out. All FAA modified solids exhibit very high activity in the polymerisation of phenol, which dominates over the hydroxylation activity. The nature of polymers formed is strongly dependent on the type and composition of the matrix applied for FAA immobilisation.

Keywords: MCM-41; AlMCM-41; NbMCM-41; Ferroceneacetic acid immobilisation; XRD; N_2 adsorption; IR; TG; Polymerisation activity

1. Introduction

Metallocenes are mostly known as catalysts for olefin polymerisation [1]. In spite of high selectivity and stereoregularity of processes conducted in homogeneous conditions [2], there are some adverse factors, which point the need of process heterogenisation. From the economical point of view, immobilisation of metallocene compounds is also profitable because it leads to the decrease of the large excess of expensive methylaluminoxane (MAO), which is used as co-catalyst. Besides, only the application of heterogeneous catalysts makes the uniform polymer particles and bulk density possible [3].

Metallocene can be also used as precursors for the preparation of metal-grafted catalysts active in the redox processes [4].

In the literature, one can find the description of three main ways for metallocene introduction into the solids. The first and the simplest route depends on immersing of support in metallocene organic solution [4,5]. The key role in this procedure plays the interaction between hydroxyl groups of the solid with supported material. For the sake of this, the process is usually preceded by surface activation. The second route consists in coverage of solid surface with methylaluminoxane (MAO). On that pre-treated support the metallocene is introduced [6]. In the last route the cyclopentadienyl ligands are immobilised first. The metal compound is introduced afterwards from its salt solution [7].

Especially attractive supports for metallocene are mesoporous molecular sieves of M41S family discovered in 1992 [8]. MCM-41 and MCM-48 belonging to this family represent very high surface area and pore volume, which makes the introduction of bulky metallocene molecules easy. These types of materials are especially addressed to the catalytic liquid phase processes [9] due to the reduction of diffusion limitation and relatively easy isomorphous substitution of transition metals.

The aim of this study was to use a simple way of ferrocene immobilisation in MCM-41 type materials and characterise the physicochemical properties of the obtained materials. We introduced ferroceneacetic acid (FAA) directly onto mesoporous materials of MCM-41 type, which contained various heteroatoms: aluminium (AlMCM-41) or niobium (NbMCM-41). A choice of heteroatoms based on the literature data, which indicate that one of the role of

* Corresponding author. Tel.: +48 61 829 1243; fax: +48 61 865 8008.
E-mail address: ziolek@amu.edu.pl (M. Ziolek).

0920-5861/$ – see front matter © 2005 Elsevier B.V. All rights reserved.
doi:10.1016/j.cattod.2005.01.007

MAO added as co-catalyst were the formation of three-coordinated Al species—a possible adsorption sites for metallocene [10]. Generally, MAO makes the introduction of metallocene easier and there is no doubt that aluminium plays an important role in the catalytic processes carried out on metallocene-based catalysts. Therefore, aluminosilicate (AlMCM-41) might be an attractive support for ferrocene. The other matrix, NbMCM-41, was chosen due to the literature data [5] concerning the immobilisation of ferrocene on niobia grafted on silica. The authors have found the oxidative properties of the prepared catalysts. It is important to stress that both AlMCM-41 and NbMCM-41 materials exhibit Lewis acidity [11] which can be important in the consideration of co-catalyst role. To get to know how mesoporous structure influences the surface and catalytic properties, the similar catalysts based on amorphous silica were prepared and characterised. The catalysts were tested in the reaction of phenol with hydrogen peroxide and isopropanol decomposition. The catalytic activity was compared with that of FeMCM-41 materials in which iron was introduced during the synthesis [12].

2. Experimental

2.1. Synthesis

For the preparation of MCM-41, AlMCM-41 and NbMCM-41 materials the classical hydrothermal synthesis in the polypropylene (PP) bottles has been applied [8,13]. Synthesis was carried out in the presence of cetyltrimethylammonium cations (CTA^+) from mixtures containing salts of aluminium or niobium and silica source. The reactant mixture consisted of sodium silicate (27% SiO_2 in 14% NaOH) for MCM-41 material, and appropriate amounts of aluminium sulphate and niobium(V) oxalate for AlMCM-41 and NbMCM-41 materials, respectively. The ratios of Si/Al or Si/Nb in the gel were assumed as 32. The formed gel from these components was stirred for 0.5 h. Next, the pH was adjusted to 11, and distillate water was added. The gel was moved into a PP bottle and heated without stirring at 373 K for 24 h. The reactants were cooled down to RT in order to adjust pH again to 11. After this, the mixture was heated once more to 373 K and left for another 24 h. The product was filtrated and washed with distilled water. After drying, the template was removed by calcination at 823 K (temperature ramp 5 K/min), 1 h in helium flow and 15 h in air under static conditions.

Fe containing MCM-41 materials were prepared in the same way. Iron(III) nitrate was used as Fe source. The assumed Si/Fe ratio was 64 (FeMCM-41-64) or 128 (FeMCM-41–128). The physicochemical properties of these materials are described in [12].

In order to obtain hydrogen forms of molecular sieves, the NH_4^+ cation exchange procedure (0.1 M solution of NH_4Cl) followed by deammoniation was applied. The ammonium ions content in the solution corresponded to the number of niobium or aluminium atoms in the material. In the case of silicate MCM-41 the same concentration of solution was used. After ion exchange procedure the solid was washed with distillate water to decay of chloride ions in the filtrate. After drying at 313 K for 5 h the samples were placed in a vertical quartz reactor and dried at 673 K for 2 h under a flow of dry air.

Amorphous silica (Ventron, 99.8%) was activated for 10 h at 573 or 673 K before FAA immobilisation and it is denoted in the paper as SiO_2 573 and SiO_2 673, respectively.

2.2. Ferroceneacetic acid (FAA) immobilisation

The simple method for immobilisation of FAA has been applied. The introduction of FAA was carried out by immersing the solid material (1 g of silica or mesoporous material) into 100 cm^3 of toluene solution of FAA. The content of FAA molecules in the solution corresponded to the number of niobium or aluminium atoms in the material. In the case of siliceous MCM-41 or amorphous silica the same concentration of solution was used. The mixture was stirred at room temperature for 3 h. Next, the solid was separated from the solution by filtration and washed with 200 cm^3 of toluene. At the end, the catalyst was dried at 353 K for 10 h.

2.3. Characterisation

X-ray diffraction patterns were recorded on a TUR-62 diffractometer (Cu Kα radiation; $\lambda = 0.154$ nm) with a step of 0.02°.

The surface area and pore volume of the materials were measured by nitrogen adsorption/desorption at 77 K using the conventional technique on a Micromeritisc 2010 apparatus. Prior to the adsorption measurements, the samples were degassed in vacuum at 573 K for 2 h. Surface area was calculated by the BET method. The PSD, the pore size (the maximum of PSD) and the mesopore volume were determined from the adsorption isotherms using the corrected algorithm (KJS–BJH) based on the Barred–Joyner–Helenda (BJH) procedure [14].

The infrared spectra were recorded with the Vector 22 (Bruker) spectrometer. The pressed wafers of the materials were placed in the vacuum cell and activated at RT for 6 h. All spectra were recorded at RT. Moreover, the spectra of the materials (1 mg) pressed with KBr (200 mg) were registered.

Thermogravimetry measurements were carried out in air atmosphere using SETARAM SETSYS-12 apparatus with temperature ramp 5 K/min.

2.4. Catalytic tests

Isopropanol decomposition was performed using a pulse microreactor and a helium flow of 40 $cm^3\ min^{-1}$.

The catalyst bed (0.05 g with a size fraction of $0.5 < Ø < 1$ mm) was first activated at 427 K for 2 h under helium flow (40 $cm^3\ min^{-1}$). The isopropanol conversion was studied at 473 and 523 K using 5 μl pulses of isopropanol. The reactant and reaction products were analysed using CHROM-5 gas chromatograph on line with microreactor. The reaction mixture was separate on 2 m column filled with Carbowax 400 (80–100 mesh) at 338 K in helium flow (40 $cm^3\ min^{-1}$) and detected by TC.

The phenol polymerisation and hydroxylation with hydrogen peroxide was carried out in a glass flask equipped with a magnetic stirrer, a thermocouple, a reflux condenser, and a membrane for sampling. The process was performed in the liquid phase using distillate water as a reaction medium. The reaction conditions were as follows: the reaction temperature – 333 K; the reaction mixture consisted of 13 g of phenol + 8 g of water + 0.2 g of the catalyst + ∼30% aqueous solution of H_2O_2 (25 mol% in relation to phenol, dropwise addition for 1 h 40 min). The process was continued for 1 h at 333 K after the admission of hydrogen peroxide. HPLC (Waters) was applied for analyses of the reaction mixtures at the following conditions: column – MACHEREY-NAGEL, Nucleosil 100-5; Protect – 1.5 μm; $L = 250$ nm; diameter – 4.6 mm; loop size – 5 μl; temperature of the column – ∼298 K (room temperature); UV detector.

3. Results and discussion

3.1. Physicochemical characterisation

The modification procedure slightly influences the structure/texture parameters of MCM-41 type materials. XRD patterns presented in Fig. 1 are consistent with the X-ray powder diffraction patterns of silicate MCM-41 reported in the literature. They are characterised by a narrow single peak (1 0 0) centred at $2\theta \approx 2^\circ$ and up to three signals

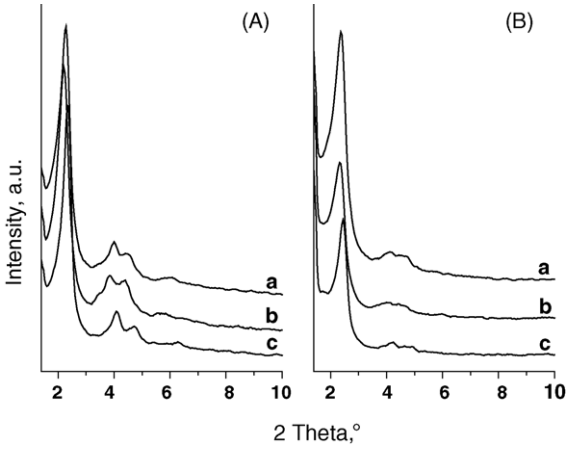

Fig. 1. XRD patterns before (A) and after (B) immobilisation of FAA on: (a) AlMCM-41; (b) MCM-41; (c) NbMCM-41.

in the region of $2\theta = 3$–8°. The latter are due to the ordered hexagonal array of parallel mesoporous tubes. After FAA immobilisation in all MCM-41 materials the XRD reflexes in this region are less resolved than those in the parent samples suggesting a partial loss in a long range order (Fig. 1(B)) [15] or rather the partial filling of mesopores with FAA. The latter case is confirmed by the broadening of reflexes at $2\theta \approx 2^\circ$ after FAA immobilisation.

The nitrogen adsorption/desorption isotherms shown in Fig. 2 are of type IV in the IUPAC classification and exhibit a distinct feature: a sharp capillary condensation step at a relative pressure of ∼0.35. The sharpness of the steep rise is diminished as a result of FAA immobilisation (compare Fig. 2(A) and (B)). The hysteresis loop in the p/p_0 range close to the saturation pressure ($p/p_0 = 0.9$–1.0) is untouched after FAA modification. Contrary, the size of the other hysteresis loop in $p/p_0 = 0.5$–0.9 range, characteristic of NbMCM-41 support, decreases after FAA incorporation. This hysteresis loop is caused by the presence of the defect holes in the mesoporous material [12,16]. Recently [17], it has been found that niobium species are located in these defect holes. The change in this hysteresis loop demonstrated in Fig. 2 suggests that ferroceneacetic acid interacts with niobium species located in the holes.

The data calculated from N_2 adsorption isotherm are shown in Table 1. One can notice that in the case of mesoporous materials all textural parameters, except wall thickness, decrease after FAA incorporation. The surface BET area is still relatively high (920–990 $m^2\ g^{-1}$) in ferroceneacetic acid modified samples. The increase of the wall thickness indicates the immobilisation of FAA into the matrix. Based on these data one can conclude that FAA species are partially located in the mesoporous walls.

FT-IR spectra allow us to conclude that hydroxyl groups participate in the immobilisation of FAA. It is demonstrated in Fig. 3. The spectrum of pure silica before FAA immobilisation exhibits one sharp band at 3747 cm^{-1}, assigned to isolated terminal silanols, and two broad bands in the range of 3650–3400 cm^{-1} due to hydrogen bonded silanol groups. The intensity of the latter bands depends on the activation temperature (Fig. 3(A)(a) and (B)(a)). The intensity of hydroxyl band at 3747 cm^{-1} considerably decreases after modification of the support with FAA. This phenomenon can by explained by the chemical interaction of surface OH groups with FAA. It results in the growth of hydrophobic properties of the catalyst, important in many liquid phase oxidation processes [e.g. [9]]. Similar results were obtained for mesoporous matrices. The participation of silanol groups in FAA immobilisation process is also supported by the impact of activation temperature of the matrix before FAA addition on the amount of iron in the final samples. The higher activation temperature of the support the lower amount of FAA is located in the final material (the example for silica is given in Table 1). The immobilisation of FAA on mesoporous MCM-41 type materials exhibiting very high surface areas is much higher than on silica. In the

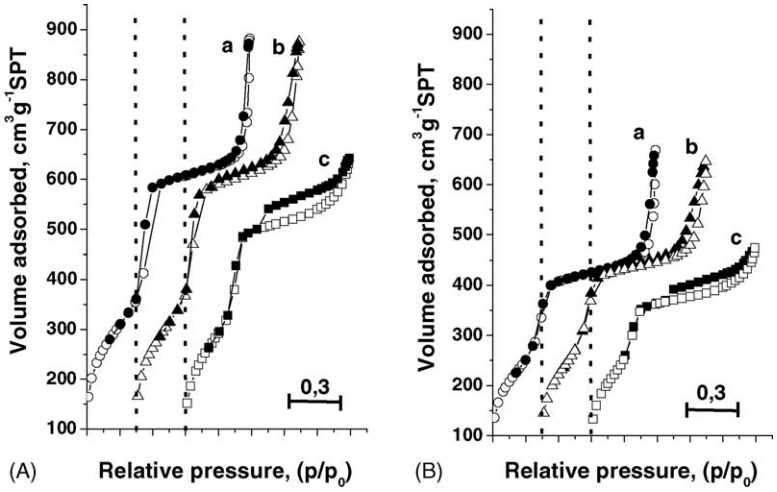

Fig. 2. N_2 adsorption/desorption isotherms at 77 K before (A) and after (B) immobilisation of FAA species on: (a) MCM-41; (b) AlMCM-41; (c) NbMCM-41.

Table 1
The characterisation of the catalysts used in this study

Catalysts	Fe content (wt.%)	BET surface area ($m^2\ g^{-1}$)	Wall thickness (t, nm)[b]	Mesopore volume (KJS[c], $cm^3\ g^{-1}$)	Pore diameter (KJS[c], nm)
MCM-41	–	1130	0.77	1.04	4.15
AlMCM-41	–	1150	0.69	1.14	3.95
NbMCM-41	–	1080	0.77	0.95	3.63
FAA/MCM-41	1.81	920	0.94	0.74	3.36
FAA/AlMCM-41	1.96	990	0.86	0.81	3.35
FAA/NbMCM-41	1.89	930	0.96	0.67	3.07
FAA/SiO_2 (573)[a]	1.20	320	–	–	–
FAA/SiO_2 (673)[a]	0.37	320	–	–	–

[a] Activation temperature.
[b] $t = a_0 - w/1.05$; $a_0 = 2d_{100}\frac{1}{\sqrt{3}} = 1.154700538d_{100}$; $w = \sqrt{\frac{8}{\sqrt{3}\pi}}d_{100}\sqrt{\frac{\rho V}{1+\rho V}} = 1.212522325d_{100}\sqrt{\frac{\rho V}{1+\rho V}}$.
[c] Calculated according to Kruk, Jaroniec, Sayari (KJS) method [14].

presence of Al or Nb in the support the hydroxyl groups bounded to these metal species or metallic cations take also part in the FAA immobilisation. This behaviour is considered below (Fig. 4) on the basis of FT-IR study in 1400–1800 cm^{-1} range.

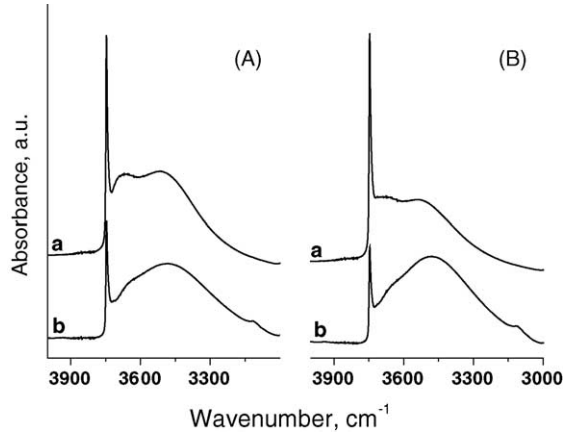

Fig. 3. FT-IR spectra recorded after evacuation for 6 h at RT before (a) and after (b) FAA immobilisation on: (A) SiO_2 573; (B) SiO_2 673.

Besides the activation temperature, the nature of heteroatoms in mesoporous molecular sieves influences FAA immobilisation. The presence of Al or Nb in the mesoporous matrix favours the higher FAA coverage (AlMCM-41 > NbMCM-41 > MCM-41 from Table 1). Infrared spectra of the samples (pressed with KBr) allow the estimation of the form of FAA adsorbed on MCM-41 materials. The example is given in Fig. 4 for aluminosilicate AlMCM-41 support. The free FAA complex (Fig. 4a) shows, among others, two absorption bands at 1713 and 1434 cm^{-1} due to the asymmetric and symmetric ν(COO) stretching modes, respectively. They are not visible at the same positions in the IR spectrum of FAA/AlMCM-41 (Fig. 4b). However, the spectrum of FAA immobilised on AlMCM-41 exhibits two new, not well-resolved, bands in the 1450–1500 cm^{-1} region. They represent symmetric ν(COO) shifted to the higher wavenumbers. Compared to the free FAA, a decrease of the energy between asymmetric and symmetric ν(COO) stretching modes is observed. This usually occurs in the case when the carboxylate groups are coordinated to a metal as a bidentate ligand. The same phenomenon was observed by Pessoa et al. [5] who

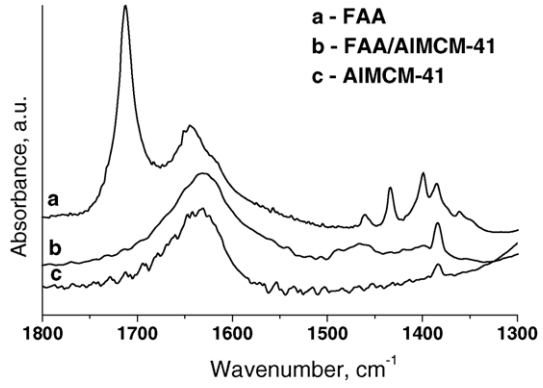

Fig. 4. FT-IR spectra of AlMCM-41, FAA/AlMCM-41 and free FAA (1 mg samples mixed with 200 mg KBr).

immobilised ferrocenecarboxylic acid on niobia grafted on silica.

Thermogravimetric studies did not indicate the significant difference in thermal stability of FAA immobilised on various matrices. Fig. 5 shows TG, DTG and DTA curves for the catalysts studied. DTG curve is included only for one sample (FAA/NbMCM-41) to make the figures more clear. All the materials exhibit one endothermic peak below 373 K accompanied by a loss of weight. It corresponds to the desorption of physically adsorbed water. The weight loss indicates that the amount of physisorbed water is much lower on SiO_2 matrix than that on mesoporous supports, as one can expect. Moreover, an exothermic peak at 588 K (FAA/MCM-41), 585 K (FAA/AlMCM-41 and FAA/NbMCM-41) and 580 K (FAA/$SiO_2$573) is accompanied by the loss of weight and is detected in all materials. It is typical of organic compounds burning. There is not a significant difference (below 10 K) in the temperature of the maximum of this peak depending on the nature of the support. However, even so small difference allows us to, suppose that thermal stability of ferrocene species is higher on mesoporous matrices (588 K for FAA/MCM-41) than on amorphous silica (580 K for FAA/$SiO_2$573). One cannot exclude that the higher temperature of exothermic peak is

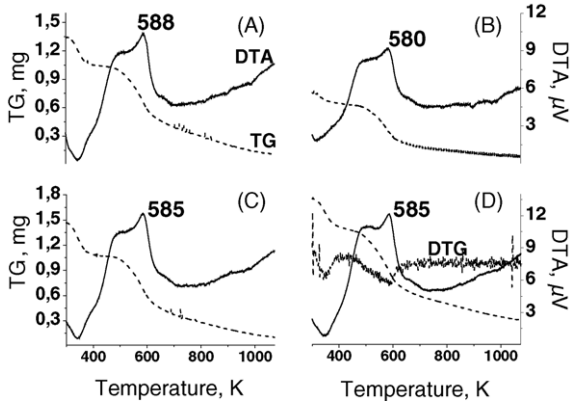

Fig. 5. DTA–TG–DTG profiles of: (A) FAA/MCM-41; (B) FAA/$SiO_2$573; (C) FAA/AlMCM-41; (D) FAA/NbMCM-41.

caused by the diffusion effect in the mesoporous tubes, which causes the shift of the temperature maximum. The discussed exothermic peak is preceded by another characterised by a broad shoulder at ~500 K which can be caused by the decomposition of ferrocene species and evaporation of light components and most probably covered by the gradually dehydroxylation of the support. This feature is characteristic for all the materials modified with FAA but less pronounced for the free ferroceneacetic acid in which dehydroxylation process does not occur (not shown in the figure).

3.2. Catalytic activity

3.2.1. Isopropanol decomposition

The isopropanol decomposition is a test reaction for the characterisation of acidic (Brønsted or Lewis) and/or basic properties of the solids [18]. Dehydration of alcohol to propene and/or di-isopropyl ether requires acidic centres, whereas the dehydrogenation to acetone occurs on basic sites. Some authors [e.g. [19]] have stated that acetone formation takes place on redox centres.

The conversion of isopropanol and the selectivity to products are shown in Table 2. As one can expect, the conversion of isopropanol before FAA incorporation is negligible. Only the traces of propene were detected at both temperatures. The presence of FAA in the materials does not make the conversion considerably higher at 473 K, but the distribution of products changes. For the same iron content in amorphous silica (prepared by the impregnation with Fe(III) nitrate), at this temperature, the conversion of isopropanol was about 34% with selectivity to propene 91% and to ether 8% [20]. It clearly shows the completely different iron properties of Fe/SiO_2 in comparison to FAA modified materials. The same is true for the sample in which iron was incorporated into the mesoporous walls during the synthesis (FeMCM-41-128; Si/Fe = 128). Although its activity is much lower than that of Fe/SiO_2 and comparable with that of FAA/MCM-41 the selectivity to acetone is negligible. The FAA containing materials demonstrate the higher redox/basic behaviour, which is manifested in selectivity to acetone (~50% at 473 K). The increase of temperature makes the isopropanol conversion higher which is typical of reactions performed in the kinetic region. The increase in conversion is accompanied by the selectivity changes. This fact can be caused to some extent by a partial FAA decomposition, and creation of other iron centres, for example iron oxide particles. Decomposition of the FAA species was confirmed by thermogravimetry measurements. However, one should point out that selectivity generally depends on the conversion level.

3.2.2. Reactions of phenol (hydroxylation and polymerisation)

The reaction of isopropanol indicates the redox activity of samples modified with ferrocene. In order to estimate the

Table 2
The results of *i*-PrOH decomposition

Catalysts	Temperature (K)	*i*-PrOH conversion (%)	Selectivity (%)		
			Propene	Ether	Acetone
MCM-41	473	~0.05	100	–	–
	523	~0.05	100	–	–
FAA/MCM-41	473	0.20	47	–	53
	523	1.80	72	–	28
NbMCM-41	473	~0.07	100	–	–
	523	~0.07	100	–	–
FAA/NbMCM-41	473	0.45	44	–	56
	523	5.80	94	–	6
FeMCM-41-128	523	3.00	84	14	2
Fe/SiO_2[a]	473	34.00	91	8	1

[a] From [20].

redox properties in the liquid phase the hydroxylation of phenol with ~30% hydrogen peroxide in water as the reaction medium was performed. The obtained results are shown in Table 3. This table contains also the results of the reaction carried out in the homogeneous system (FAA in aqueous solution) and in the heterogeneous one (FAA/AlMCM-41 used as the catalyst) without the use of hydrogen peroxide. Moreover, the activity of iron containing mesoporous sieves in which Fe was introduced during the synthesis (FeMCM-41 and FeNbMCM-41) is exhibited.

One can notice a very high consumption of phenol (96.5 wt.%) on MCM-41 type materials modified with FAA. There is no support impact on the conversion level. Regarding the hydroxylation conditions which were used, only 25 wt.% of phenol was able to react with H_2O_2. Hundred percent of H_2O_2 was converted (with the exception of FAA/NbMCM-41 – 98%), whereas, there were only traces of hydroxylation products. It indicates that another process (processes) has to be responsible for a loss of phenol. Moreover, too fast decomposition of hydrogen peroxide makes the hydroxylation process less effective. It suggests that the catalysts modified with FAA are highly active in the other process than the hydroxylation reaction. This phenomenon is supported by the reaction carried out in the absence of H_2O_2. As one could expect, there was no hydroxylation products detected after the reaction in this case, but the conversion of phenol was also very high (only 3 wt.% lower than in the presence of hydrogen peroxide).

In spite of the facts mentioned above, it is worth to note that hydroxylation of phenol in the presence of niobium in mesoporous material led to the lack of catechol in the post-reaction mixture. This behaviour was also observed on the samples in which iron was incorporated into mesoporous material during the synthesis together with niobium (FeNbMCM-41 material) and this feature was accompanied by a very low hydroxylation activity. The hydroxylation process was more evidenced when FeMCM-41 sample was used as the catalyst. In the case of both catalysts prepared via Fe introduction during the synthesis, the phenol conversion was about four times lower than that found on FAA modified samples.

One could suppose that the polymerisation process could be responsible for the loss of phenol mass after the reaction. For the insight into eventually creation of polymers, the thermogravimetric measurements have been applied. Fig. 6 exhibits the TG and DTA curves, obtained in air atmosphere, for the materials after the reaction. Moreover, the data for heating of pure phenol are shown in Fig. 7. The latter indicates two endothermic effects at 318 and 430 K. The first one is due to the transformation of phenol to a liquid state

Table 3
Phenol and hydrogen peroxide conversion and selectivity to hydroxylation products

Catalysts	H_2O_2 conversion (%)	Phenol conversion		Phenol conversion (g) to	
		g	%	Catechol	Hydroquinone
FAA[a]	100	12.5	96.5	0.05	0.03
FAA/SiO2573	100	12.5	96.5	0.05	0.02
FAA/MCM-41	100	12.5	96.5	0.04	0.02
FAA/NbMCM-41	98	12.5	96.5	0	0.01
FAA/AlMCM-41	100	12.5	96.5	0.05	0.03
FAA/AlMCM-41[b]	–	12.1	93.5	0	0
FeMCM-41-128	100	3.6	28	0.82	0.43
FeNbMCM-41-64	100	3.1	24	0	0.04

[a] Reaction in homogeneous condition.
[b] Reaction in the absence of H_2O_2.

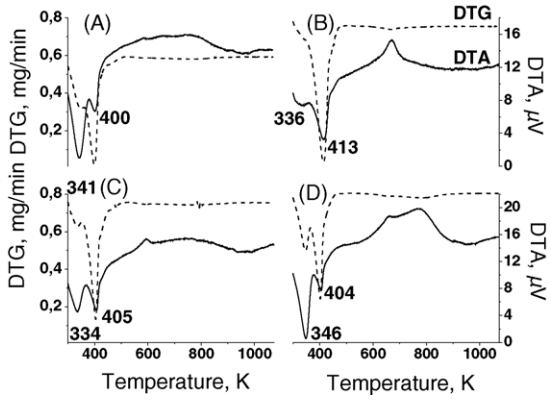

Fig. 6. DTA–TG profiles of: (A) FAA/MCM-41, (B) FAA/$SiO_2$573, (C) FAA/AlMCM-41 and (D) FAA/NbMCM-41 after the reaction of phenol with hydrogen peroxide.

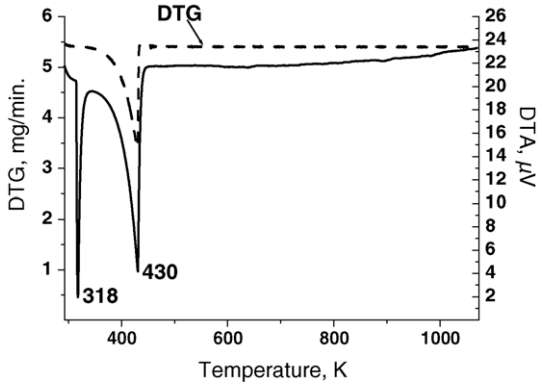

Fig. 7. DTA–TG profiles of phenol.

and the second, accompanied by the weight loss, is caused by phenol evaporation. The peak from phenol evaporation is present in thermogravimetric curves of all the materials after the reaction. It appears at ca. 400–413 K, depending on the sample (Fig. 6). The temperature and the weight loss are determined by the amount of residual phenol. It is the lowest in case of FAA/MCM-41. The first endothermic peak at 334–346 K origins from the desorption of water. It is accompanied by the weight loss and it can cover the sharp peak due to phenol melting. The gradually increasing exothermic effects in the range between 600 and 900 K accompanied by the weight loss can be assigned to oxidation of polymers. They are not detected when thermogravimetric measurements are performed in helium atmosphere (not shown in the figure). The shape of DTA curves indicates various compositions (weight) of the created polymers depending on the nature of matrix for FAA. Taking into account the loss of weight, above 500 K, one can estimate the highest polymer production on FAA/NbMCM-41. It is worth to note that the presence of exothermic effect at ca. 584 and 594 K shows that ferrocene species is still present on the catalyst surface after the reaction and it is oxidised at these temperatures. This behaviour supports the heterogeneous character of the polymerisation process as well as the stability of ferrocene species on the support. The exothermic peak at ~590 K is not visible on DTA curves of FAA/NbMCM-41 and FAA/SiO_2 after the reaction. It can be covered by the increase of a base line caused by exothermic oxidation of polymer. However, it can be also caused by a partial leaching of ferrocene species to the solution. The solutions after the reaction have not been examined for iron content, due to the presence of phenol, which makes AAS analysis impossible. Therefore, one cannot exclude that polymerisation process partly occurs in the solution (homogeneous system). However, the difference in the nature of products depending on the type of solid catalysts indicates the participation of the heterogeneous catalysts in this process. The observed phenomena require the further detailed study which will be undertaken. In this paper we wish to point out the advantages of various mesoporous matrices for FAA in the creation of attractive heterogeneous polymerisation catalysts.

4. Summary

A simple method for immobilisation of ferroceneacetic acid (FAA) applied in this study is easy and effective technique for the modification of physicochemical properties of mesoporous MCM-41 materials. The FAA loading is higher in the case of mesoporous materials than on amorphous silica, and the presence of aluminium or niobium in the framework enhances FAA coverage. The modification procedure slightly influences the structural/textural properties of the support. The FT-IR study exhibits the participation of surface OH groups in the process of FAA incorporation. The increase of wall thickness in MCM-41 materials indicates FAA immobilisation into the solid. Moreover, the change in the size of hysteresis loop in nitrogen adsorption/desorption isotherm of NbMCM-41 resulted from FAA immobilisation suggests the interaction between niobium species located in the defect holes and FAA.

FAA modified materials show a redox behaviour, which is manifested by the selectivity to acetone in the isopropanol dehydrogenation. However, the activity of these catalysts in this reaction is negligible. All samples containing ferrocene species exhibit high activity in phenol polymerisation process. The types of polymers formed are determined by the nature of the mesoporous support applied for FAA immobilisation.

Acknowledgments

The authors appreciate Mr. M. Gedziorowski's excellent contribution in the experimental work. State Committee for Scientific Research (KBN grant no. 3T09A 09626; 2004–2005) is acknowledged for financial support. Acknowledge is made to CBMM (Brasil) for supplying niobium(V) oxalate.

References

[1] G.G. Hlatky, Coord. Chem. Rev. 181 (1999) 243.
[2] K.-S. Lee, C.-G. Oh, J.-H. Yim, S.-K. Ihm, J. Mol. Catal. A 159 (2000) 301.
[3] M. Michelotti, G. Arribas, S. Bronco, A. Altomare, J. Mol. Catal. A 152 (2000) 167.
[4] K.K. Kang, W.S. Ahn, J. Mol. Catal. A 159 (2000) 403.
[5] C.A. Pessoa, Y. Gushikem, L.T. Kubota, Electrochem. Acta 46 (2001) 2499.
[6] P.G. Belelli, M.L. Ferreira, D.E. Damiani, Appl. Catal. A 228 (2002) 189.
[7] A.M. Uusitalo, T.T. Pakkanen, E.L. Iskola, J. Mol. Catal. A 177 (2002) 179.
[8] J.S. Beck, J.C. Vartuli, W.J. Roth, M.E. Leonowicz, C.T. Kresge, K.D. Schmitt, C.T.-W. Chu, D.H. Olson, E.W. Sheppard, S.B. McCullen, J.B. Higgins, J.L. Schlenker, J. Am. Chem. Soc. 114 (1992) 10834.
[9] M. Ziolek, Catal. Today 90 (2003) 145.
[10] A.-M. Uusitalo, T.T. Pakkanen, M. Kroger-Laukkanen, L. Niinisto, K. Hakala, S. Paavola, B. Lofgren, J. Mol. Catal. A 160 (2000) 343.
[11] M. Ziolek, I. Nowak, J.C. Lavalley, Catal. Lett. 45 (1997) 259.
[12] M. Ziolek, I. Nowak, B. Kilos, I. Sobczak, P. Decyk, M. Trejda, J.C. Volta, J. Phys. Chem. Solids 65 (2004) 571.
[13] M. Ziolek, I. Nowak, Zeolites 18 (1997) 356.
[14] M. Kruk, M. Jaroniec, A. Sayari, Langumir 13 (1997) 6267.
[15] T. Blasco, A. Corma, M.T. Navarro, J/P. Pariente, J. Catal. 159 (1995) 65.
[16] H.-P. Lin, S.-T. Wong, Ch.-Y. Mou, Ch.-Y. Tang, J. Phys. Chem. B 104 (2000) 8967.
[17] B. Kilos, M. Aouine, I. Nowak, M. Ziolek, J.C. Volta, J. Catal. 224 (2004) 314.
[18] A. Gervasisni, J. Fenyvesi, A. Auroux, Catal. Lett. 43 (1997) 219.
[19] C. Lahausse, J. Bechelier, J.C. Lavalley, H. Lauron-Pernot, A.M. Le Govic, J. Mol. Catal. 87 (1994) 329.
[20] P. Decyk, M. Trejda, M. Ziolek, J. Kujawa, K. Glaszczka, M. Bettahar, S. Monteverdi, M. Mercy, J. Catal. 219 (2003) 146.